

Pion photoproduction amplitude relations in the $1/N_c$ expansion

Thomas D. Cohen* and Daniel C. Dakin†

Department of Physics, University of Maryland, College Park, Maryland 20742-4111, USA

Richard F. Lebed‡ and Daniel R. Martin§

Department of Physics and Astronomy, Arizona State University, Tempe, Arizona 85287-1504, USA

(Received 4 January 2005; published 19 April 2005)

We derive expressions for pion photoproduction amplitudes in the $1/N_c$ expansion of QCD, and obtain linear relations directly from this expansion that relate electromagnetic multipole amplitudes at all energies. The leading-order relations in $1/N_c$ compare favorably with available data, while the next-to-leading-order relations seem to provide only a small improvement. However, when resonance parameters are compared directly, the agreement at $O(1/N_c)$ or $O(1/N_c^2)$ is impressive.

DOI: 10.1103/PhysRevD.71.076010

PACS numbers: 11.15.Pg, 13.60.Le

I. INTRODUCTION

A recent paper [1] presented the derivation of linear relationships among partial-wave amplitudes for $\pi N \rightarrow \pi N$ and $\pi N \rightarrow \pi \Delta$ that hold in large N_c QCD with only $O(1/N_c^2)$ corrections. They were obtained using a model-independent formalism based upon the group structure of the contracted SU(4) spin-flavor symmetry that emerges in the single-baryon sector as $N_c \rightarrow \infty$; this symmetry by construction ensures consistent N_c power counting for baryon-meson scattering processes [2–4]. The formalism of Ref. [1] allows for the inclusion of systematic $1/N_c$ corrections to leading-order results [5] among S matrix elements, specifically the partial-wave amplitudes. From this expansion one may obtain linear amplitude relations that hold to $O(1/N_c^2)$. As expected, available data support these predictions better than ones holding only to $O(1/N_c)$ [1].

The approach for deriving πN scattering relations can be applied to other processes, including single-nucleon Compton scattering, electron scattering, pion electroproduction ($\gamma^* N \rightarrow \pi N$) and photoproduction ($\gamma N \rightarrow \pi N$). In this paper we focus on pion photoproduction, for which the relevant experimentally accessible quantities are the electromagnetic multipole amplitudes $M_{L\pm}$ and $E_{L\pm}$. We present relations among these multipole amplitudes that hold to leading order (LO) and next-to-leading order (NLO) in $1/N_c$ [6].

Relations among pion photoproduction amplitudes are not new. They can be derived using models in which baryons are considered as chiral solitons, such as the Skyrme model [7,8]; the group-theoretical aspects of these models find justification in large N_c QCD, as discussed in Refs. [9,10]. However, the calculations in Refs. [7,8] do not employ large N_c QCD as a constraint; the relations obtained there represent a conglomerate of terms appearing at

different orders in $1/N_c$, as discussed in Sec. II. Consequently, the relations in Refs. [7,8] are not results of the $1/N_c$ expansion.

In this paper, we derive a model-independent expansion for electromagnetic multipole amplitudes in terms of model-dependent functions whose coefficients are fixed by group theory. As shown in Sec. III, these model-dependent functions can be algebraically eliminated to yield seven model-independent linear relations. These are compared with experimental data in Sec. IV. We summarize in Sec. V.

We begin by considering general processes of the form $\Phi_1 + B_1 \rightarrow \Phi_2 + B_2$, where B_1 and B_2 are incoming and outgoing nonstrange baryons, and Φ_1 and Φ_2 are incoming and outgoing nonstrange mesons, respectively. It is also possible to generalize to scattering processes in which each pair B_1 and B_2 , and Φ_1 and Φ_2 , have a fixed nonzero strangeness [11]. Amplitude relations for these processes were first noted in the context of chiral soliton models [12], then as model-independent group-theoretical results derived from a solitonic picture related to the large N_c limit in Refs. [13,14], and finally as true model-independent results of the $1/N_c$ expansion in Ref. [5]. The derivation of the multipole amplitudes for pion photoproduction is similar to those of Refs. [5,14], except that Φ_1 now represents a photon rather than a meson (or technically, a meson interpolating field with the quantum numbers of a photon). Although photons are spin 1, one precombines the photon spin with its orbital angular momentum relative to the nucleon target to give the usual multipole angular momentum [15] in scattering processes involving radiation. With this in mind, one begins with the master expression for meson-baryon partial-wave amplitudes from Refs. [5,14]:

$$S_{L_i L_f S_i S_f I J} = \sum_{K, \tilde{K}_i, \tilde{K}_f} [K]([R_i][R_f][S_i][S_f][\tilde{K}_i][\tilde{K}_f])^{1/2} \times \begin{Bmatrix} L_i & i_i & \tilde{K}_i \\ S_i & R_i & s_i \\ J & I & K \end{Bmatrix} \begin{Bmatrix} L_f & i_f & \tilde{K}_f \\ S_f & R_f & s_f \\ J & I & K \end{Bmatrix} \tau_{K \tilde{K}_i \tilde{K}_f L_i L_f} \quad (1.1)$$

*Electronic address: cohen@physics.umd.edu

†Electronic address: dcdakin@physics.umd.edu

‡Electronic address: Richard.Lebed@asu.edu

§Electronic address: daniel.martin@asu.edu

where the *reduced amplitude* τ is a model-dependent function that depends only on energy and the quantum numbers $\{K, \tilde{K}_i, \tilde{K}_f, L_i, L_f\}$. Its explicit form can be found only after a particular model of nucleon dynamics, such as the Skyrme model, is specified. The notation $[X]$ is shorthand for $2X + 1$, the dimension of the spin- X SU(2) representation.

The quantum numbers specified in Eq. (1.1) include the initial (final) spin-isospin of the nucleon R_i (R_f), which combines vectorially with the initial (final) meson spin s_i (s_f) to give the total intrinsic spin of the system S_i (S_f). These in turn combine with the initial (final) meson-baryon relative orbital angular momenta L_i (L_f) to give the total angular momentum J . The initial (final) meson isospin i_i (i_f) combines with the nucleon isospin to give the total isospin I . The effect of constraints from the $1/N_c$ expansion is that the grand spin $\mathbf{K} \equiv \mathbf{I} + \mathbf{J}$ and the hybrid quantities $\tilde{\mathbf{K}}_i \equiv \mathbf{i}_i + \mathbf{L}_i$ and $\tilde{\mathbf{K}}_f \equiv \mathbf{i}_f + \mathbf{L}_f$ provide good quantum numbers K, \tilde{K}_i , and \tilde{K}_f . The sums in Eq. (1.1) then run over all values consistent with the $9j$ symbols, meaning that the entries in each row and column satisfy a triangle rule.

In using Eq. (1.1) to describe the process $\gamma N \rightarrow \pi N$, the precombination of photon intrinsic spin with orbital angular momentum relative to the nucleon target into a multipole field of order ℓ is represented by a simple mathematical expedient: One sets $s_i = 0$ and $L_i = \ell$ in the first $9j$ symbol. Since ℓ represents the total of both sources of angular momentum for the photon, the intrinsic spin of the photon may effectively be set to zero. As a side note, the same trick would work for pion electroproduction, where the photon is virtual and can also couple through its spin-0 piece.

One important complication must be dealt with before applying Eq. (1.1) to photoproduction processes: The photon has both isoscalar and isovector pieces. In large N_c QCD, the leading isovector coupling of a photon to a ground-state nucleon enters through the combined spin-flavor operator

$$G^{ia} \equiv \sum_{\alpha=1}^{N_c} q_{\alpha}^{\dagger} \left(\frac{\sigma^i}{2} \otimes \frac{\tau^a}{2} \right) q_{\alpha}, \quad (1.2)$$

where σ and τ are Pauli matrices in spin and isospin spaces, respectively. α sums over the N_c quark fields q_{α} in the nucleon, but it should be noted that this operator does not require a quark model to be well defined; in the field-theoretic context, q simply stands for an interpolating field with the quantum numbers of a current quark, whose effect summed over α completely exhausts the full nucleon wave function [16]. In the same language, the (spin-dependent) isoscalar coupling enters via the operator

$$J^i \equiv \sum_{\alpha=1}^{N_c} q_{\alpha}^{\dagger} \left(\frac{\sigma^i}{2} \right) q_{\alpha}. \quad (1.3)$$

The two operators differ in that the matrix elements of the former are $O(N_c^1)$ for ground-state baryons due to the collective effect of the N_c quarks, while the matrix elements of the latter are—by construction— $O(N_c^0)$ for ground-state baryons. Furthermore, since the photon couples through the quark charges, it is straightforward to see that the isovector (isoscalar) couplings have coefficients $e(q_u \mp q_d)$, respectively. If one takes the quark charges to have their usual values $q_u = +\frac{2}{3}$ and $q_d = -\frac{1}{3}$, as is done in this paper, then the relative suppression of isoscalar to isovector amplitudes is $1/N_c$. On the other hand, if one takes the point of view as in Ref. [17], where $q_u = (N_c + 1)/(2N_c)$ and $q_d = (1 - N_c)/(2N_c)$, then the isoscalar to isovector ratio becomes $1/N_c^2$ (See Ref. [18] for a fuller discussion of this point).

Equation (1.1) does not manifest this effect. Because the anomalous current coupling is suppressed in large N_c due to the difference in the origin of the isoscalar and isovector pieces, this feature does not arise in the meson scattering derivation of Refs. [5,14]. It must be put in by hand by adding to the leading isovector ($i_i = 1$) terms additional isoscalar ($i_i = 0$) terms suppressed by an explicit factor $1/N_c$. This is purely a feature of isospin breaking in the electromagnetic interaction: Both isoscalar and isovector couplings couple to the photon spin. However, a true spinless isoscalar meson (*viz.*, the η), can couple through the operator

$$\mathbb{1} \equiv \sum_{\alpha=1}^{N_c} q_{\alpha}^{\dagger} q_{\alpha}, \quad (1.4)$$

whose nucleon matrix elements are $O(N_c^1)$, and therefore couples just as strongly to nucleons as do pions through the isovector coupling Eq. (1.2).

II. DERIVATION

The derivation of the expression for pion photoproduction multipole amplitudes begins by substituting $S_i = S_f = \frac{1}{2}$, $s_i = s_f = 0$, $R_i = R_f = \frac{1}{2}$, $i_i \equiv i_f \in \{0, 1\}$ (both of which are of course added to give the full physical amplitude), and $i_f = 1$ into Eq. (1.1):

$$S_{\ell L \frac{1}{2} I J} = 2(-1)^{L-\ell} \sum_K [K] \left\{ \begin{matrix} J & \ell & \frac{1}{2} \\ i_f & I & K \end{matrix} \right\} \left\{ \begin{matrix} J & L & \frac{1}{2} \\ i_f & I & K \end{matrix} \right\} \tau_{K \ell L}. \quad (2.1)$$

From Eq. (2.1) one obtains the form of the multipole amplitudes by including the isospin Clebsch-Gordan coefficients specifying the initial and final nucleon charge states. Using ν for the pion isospin third component and m_I for that of the incoming nucleon, the multipole amplitude for a specific charge channel is

$$\begin{aligned}
 M_{\ell L J m_I \nu}^{\lambda i_\gamma} &= \begin{pmatrix} 1 & \frac{1}{2} & I \\ \nu & m_I - \nu & m_I \end{pmatrix} \\
 &\times \begin{pmatrix} i_\gamma & \frac{1}{2} & I \\ 0 & m_I & m_I \end{pmatrix} 2(-1)^{L-\ell} \sum_K [K] \\
 &\times \left\{ \begin{matrix} J & \ell & \frac{1}{2} \\ i_\gamma & I & K \end{matrix} \right\} \left\{ \begin{matrix} J & L & \frac{1}{2} \\ 1 & I & K \end{matrix} \right\} \tau_{K\ell L}^\lambda. \quad (2.2)
 \end{aligned}$$

The index λ indicates the type of multipole, and is determined by the relative parity of ℓ and L : $(\ell - L)$ odd gives electric (e) multipoles, $(\ell - L)$ even gives magnetic (m) multipoles.

This expansion is most useful when written in terms of t -channel exchange amplitudes, since large N_c QCD restricts their form as discussed in Refs. [1,19]: The leading amplitudes in $1/N_c$ have $I_t = J_t$ [14], and the amplitudes with $|I_t - J_t| = n$ are suppressed by a relative factor $1/N_c^n$. Following Ref. [1], we compute the t -channel amplitudes for the separate cases where $i_\gamma = 1$ and $i_\gamma = 0$. Using the Biedenharn-Elliot sum rule [20], one can rewrite the product of $6j$ symbols in Eq. (2.2) as

$$\begin{aligned}
 \left\{ \begin{matrix} J & \ell & \frac{1}{2} \\ i_\gamma & I & K \end{matrix} \right\} \left\{ \begin{matrix} J & L & \frac{1}{2} \\ i_f & I & K \end{matrix} \right\} &= \sum_J \frac{(-1)^{2J-i_f+i_\gamma} [J]}{2\sqrt{[i_f][i_\gamma][L][\ell]}} \\
 &\times \begin{bmatrix} i_f & L & K \\ \ell & i_\gamma & J \end{bmatrix} \\
 &\times \begin{bmatrix} i_f & \frac{1}{2} & I \\ \frac{1}{2} & i_\gamma & J \end{bmatrix} \\
 &\times \begin{bmatrix} L & \frac{1}{2} & J \\ \frac{1}{2} & \ell & J \end{bmatrix}, \quad (2.3)
 \end{aligned}$$

where the modified $6j$ symbols (called $[6j]$ symbols in Ref. [1]) are defined by

$$\left\{ \begin{matrix} a & b & e \\ c & d & f \end{matrix} \right\} \equiv \frac{(-1)^{-(b+d+e+f)}}{([a][b][c][d])^{1/4}} \left[\begin{matrix} a & b & e \\ c & d & f \end{matrix} \right]. \quad (2.4)$$

Note that the $[6j]$ and the usual $6j$ symbols share the same triangle rules.

The full t -channel multipole amplitude can now be written in terms of $[6j]$ symbols, using Eqs. (2.2) and (2.3) with $i_f = 1$ ($[1] \rightarrow 3$) for the pion. It is convenient to define t -channel amplitudes by

$$\tau_{J\ell L}^{\lambda i_\gamma} \equiv \frac{(-1)^{2J-1+i_\gamma} [J]}{\sqrt{[1][i_\gamma][L][\ell]}} \sum_K [K] \begin{bmatrix} 1 & L & K \\ \ell & i_\gamma & J \end{bmatrix} \tau_{K\ell L}^\lambda. \quad (2.5)$$

Then, for the isovector case ($i_\gamma = 1$),

$$\begin{aligned}
 M_{\ell L J m_I \nu}^{\lambda 1} &= (-1)^{L-\ell} \begin{pmatrix} 1 & \frac{1}{2} & I \\ \nu & m_I - \nu & m_I \end{pmatrix} \\
 &\times \begin{pmatrix} 1 & \frac{1}{2} & I \\ 0 & m_I & m_I \end{pmatrix} \sum_J \left[\begin{matrix} 1 & \frac{1}{2} & I \\ \frac{1}{2} & 1 & J \end{matrix} \right] \\
 &\times \left[\begin{matrix} L & \frac{1}{2} & J \\ \frac{1}{2} & \ell & J \end{matrix} \right] \tau_{J\ell L}^{\lambda 1}. \quad (2.6)
 \end{aligned}$$

In the isoscalar case ($i_\gamma = 0$), the first $6j$ symbol and the second Clebsch-Gordan coefficient in Eq. (2.2) collapse to simple factors times Kronecker δ 's. Including the explicit $1/N_c$ suppression described above, one has

$$\begin{aligned}
 M_{\ell L J m_I \nu}^{\lambda 0} &= \frac{(-1)^{L-\ell}}{N_c} \begin{pmatrix} 1 & \frac{1}{2} & I \\ \nu & m_I - \nu & m_I \end{pmatrix} \frac{\delta_{I, \frac{1}{2}}}{[1]^{1/4}} \\
 &\times \left[\begin{matrix} L & \frac{1}{2} & J \\ \frac{1}{2} & \ell & 1 \end{matrix} \right] \tau_{1\ell L}^{\lambda 0}. \quad (2.7)
 \end{aligned}$$

Eqs. (2.6) and (2.7) are analogous to expressions obtained earlier by Eckart and Schwesinger [7], if one identifies $\tau_{K\ell L}(i_\gamma = 1)$ and $\tau_{K\ell L}(i_\gamma = 0)$ with their dynamical functions $V_{K\ell}^L(k_\gamma, k_\pi)$ and $S_{K\ell}^L(k_\gamma, k_\pi)$, respectively. Reference [7] studied photoproduction of baryon resonances in the context of the Skyrme model and derived expressions for the same multipole amplitudes as considered here. Their expansion, however, includes a third dynamical function $R_{K\ell}^L(k_\gamma, k_\pi)$ that does not appear in the present derivation, since it represents Skyrminion angular velocity terms, which vanish at leading order in $1/N_c$. Similarly, our analysis would suppress S compared to V by the aforementioned $1/N_c$ factor. The linear relations derived in Refs. [7,8] are therefore not consequences of large N_c QCD since all the functions R , S , and V are treated as equally important in their analysis.

Because of the extra $1/N_c$ suppression of isoscalar compared to isovector amplitudes, an expansion to consistent order in $1/N_c$ requires the inclusion of NLO amplitudes for just the isovector channel. We parameterize them by following the same procedure as in Ref. [1]: The LO terms all have $|I_t - J_t| = 0$ [14], while all linearly independent NLO terms have $|I_t - J_t| = 1$ [1,19]. Generalizing Eq. (2.6) in this way gives

$$\begin{aligned}
 M_{\ell L J m_I \nu}^{\lambda 1(\text{NLO})} &= \frac{(-1)^{L-\ell}}{N_c} \begin{pmatrix} 1 & \frac{1}{2} & I \\ \nu & m_I - \nu & m_I \end{pmatrix} \\
 &\times \begin{pmatrix} 1 & \frac{1}{2} & I \\ 0 & m_I & m_I \end{pmatrix} \left\{ \sum_x \left[\begin{matrix} 1 & \frac{1}{2} & I \\ \frac{1}{2} & 1 & x \end{matrix} \right] \right. \\
 &\times \left[\begin{matrix} L & \frac{1}{2} & J \\ \frac{1}{2} & \ell & x+1 \end{matrix} \right] \tau_{x\ell L}^{\lambda(+)} + \sum_y \left[\begin{matrix} 1 & \frac{1}{2} & I \\ \frac{1}{2} & 1 & y \end{matrix} \right] \\
 &\times \left. \left[\begin{matrix} L & \frac{1}{2} & J \\ \frac{1}{2} & \ell & y-1 \end{matrix} \right] \tau_{y\ell L}^{\lambda(-)} \right\}. \quad (2.8)
 \end{aligned}$$

Note that J in Eq. (2.6), and x and y in Eq. (2.8), are

dummy labels for I_t in each corresponding sum. The total multipole amplitude expansion, including all LO terms and good to consistent order in $1/N_c$, is the sum of Eqs. (2.6), (2.7), and (2.8):

$$M_{\ell L J m_I \nu}^{\lambda I} = M_{\ell L J m_I \nu}^{\lambda I 1} + M_{\ell L J m_I \nu}^{\lambda I 0} + M_{\ell L J m_I \nu}^{\lambda I 1(\text{NLO})}. \quad (2.9)$$

Some general comments apply to Eq. (2.9). First, the NLO amplitude contains only two sums since $|I_t - J_t| = 1$ is satisfied only by $I_t = J_t \pm 1$. The sum over J is constrained to 0 and 1, due to the triangle rule $\Delta(\frac{1}{2}, \frac{1}{2}, J)$ in the first $[6j]$ symbol in Eq. (2.6). Similarly, triangle rules in the second $[6j]$ symbol reduce the respective sums over x and y to single terms with $x = 0$ and $y = 1$. Equation (2.9) in its simplest expanded form, with free quantum numbers J, L, ℓ, m_I , and ν , reads

$$\begin{aligned} M_{\ell L J}^{\lambda m_I \nu} &= \sum_T (-1)^{L-\ell} \begin{pmatrix} 1 & \frac{1}{2} & I \\ \nu & m_I - \nu & m_I \end{pmatrix} \begin{pmatrix} 1 & \frac{1}{2} & I \\ 0 & m_I & m_I \end{pmatrix} \\ &\times \left\{ \delta_{\ell, L} \tau_{0LL}^{\lambda I} + \sqrt{\frac{2}{3}} \left(\delta_{I, \frac{1}{2}} - \frac{1}{2} \delta_{I, \frac{3}{2}} \right) \begin{bmatrix} L & \frac{1}{2} & J \\ \frac{1}{2} & \ell & 1 \end{bmatrix} \tau_{1\ell L}^{\lambda I} \right. \\ &+ \frac{1}{N_c} \left(\begin{bmatrix} L & \frac{1}{2} & J \\ \frac{1}{2} & \ell & 1 \end{bmatrix} \tau_{0\ell L}^{\lambda I(+)} \right. \\ &+ \left. \left. \sqrt{\frac{2}{3}} \left(\delta_{I, \frac{1}{2}} - \frac{1}{2} \delta_{I, \frac{3}{2}} \right) \delta_{\ell, L} \tau_{1LL}^{\lambda I(-)} \right) \right\} \\ &+ \frac{1}{N_c} \frac{\delta_{I, \frac{1}{2}}}{[1]^{1/4}} \begin{bmatrix} L & \frac{1}{2} & J \\ \frac{1}{2} & \ell & 1 \end{bmatrix} \tau_{1\ell L}^{\lambda 0}. \end{aligned} \quad (2.10)$$

III. LINEAR RELATIONS

Charge conservation limits the number of pion photo-production channels to four: $\gamma p \rightarrow \pi^+ n$, $\gamma n \rightarrow \pi^- p$, $\gamma p \rightarrow \pi^0 p$, $\gamma n \rightarrow \pi^0 n$. However, due to isospin invariance of the strong interaction, only three of these are independent. Since the species in $\gamma n \rightarrow \pi^0 n$ are neutral, this reaction is difficult to study experimentally and we use isospin freedom to eliminate its amplitudes (separately for total $I = \frac{1}{2}$ and $\frac{3}{2}$ channels) [21]. The remaining three charged channels can occur via an electric or magnetic transition. In the magnetic case, the photon and pion have the same orbital angular momentum ($\ell = L$), whereas in the electric case, there is a change of one unit ($\ell = L \pm 1$). Given these restrictions, the set of multipole amplitudes describing these cases can be written in terms of a still *smaller* set of reduced amplitudes. Thus one expects linear relations among the physically measurable amplitudes.

Linear relations can be derived at both LO and NLO in $1/N_c$. In order to find the LO relations, we work with only the LO pieces in Eq. (2.10) (*i.e.*, disregard the $1/N_c$ -suppressed terms). To find the relations that hold to NLO, we use the complete expression. The electric and magnetic transitions have distinct expansions and are investigated independently.

Let us begin with the expansion of the electric multipole amplitudes. Six physical amplitudes correspond to the two ways, $J = L \pm \frac{1}{2}$, of combining the pion and nucleon angular momenta for each of the three charged reactions. At LO these are expanded in terms of only two reduced amplitudes ($\tau_{1, L \pm 1, L}^{e1}$), implying four relations. Two of these are:

$$M_{L-1, L, -}^{e, p(\pi^+)n} = M_{L-1, L, -}^{e, n(\pi^-)p} + O(N_c^{-1}) \quad (L \geq 2), \quad (3.1)$$

$$M_{L+1, L, +}^{e, p(\pi^+)n} = M_{L+1, L, +}^{e, n(\pi^-)p} + O(N_c^{-1}) \quad (L \geq 0), \quad (3.2)$$

where the last subscript in each amplitude is no longer J , but represents the equivalent information of the sign in $J = L \pm \frac{1}{2}$. These relations follow simply from isospin symmetry of isovector amplitudes, since the isoscalar component of the photon current is absent at LO.

The other two LO relations imply the vanishing of the electric multipole amplitudes for $\gamma p \rightarrow \pi^0 p$ at leading order in $1/N_c$:

$$M_{L \pm 1, L, \pm}^{e, p(\pi^0)p} = O(1/N_c). \quad (3.3)$$

After extrapolating to the real world of $N_c = 3$, one expects these amplitudes to be about a factor $N_c = 3$ smaller (on average) than those of the charge-exchange reactions.

Once the NLO terms in Eq. (2.10) are included, four new reduced amplitudes ($\tau_{0, L \pm 1, L}^{te(+)}$ and $\tau_{1, L \pm 1, L}^{te0}$) appear, leaving no remaining electric multipole relations at NLO.

Turning to the magnetic transition, one sees that only two LO reduced amplitudes (τ_{1LL}^{m1} and τ_{0LL}^{m1}) are needed to describe the six physical amplitudes. This yields four LO linear relations:

$$M_{L, L, -}^{m, p(\pi^0)p} = M_{L, L, +}^{m, p(\pi^0)p} + O(N_c^{-1}) \quad (L \geq 1), \quad (3.4)$$

$$\begin{aligned} M_{L, L, -}^{m, p(\pi^+)n} &= M_{L, L, -}^{m, n(\pi^-)p} = -\frac{L+1}{L} M_{L, L, +}^{m, p(\pi^+)n} \\ &= -\frac{L+1}{L} M_{L, L, +}^{m, n(\pi^-)p} \quad (L \geq 1). \end{aligned} \quad (3.5)$$

As before, two of these follow from isospin symmetry among the isovector amplitudes. The NLO terms bring in only three more reduced amplitudes ($\tau_{0LL}^{tm(+)}$, $\tau_{1LL}^{tm(-)}$, and τ_{1LL}^{tm0}), meaning that one relation remains at this order. Indeed, one might have anticipated fewer amplitudes in the magnetic rather than the electric transition since, in the former case, only $\ell = L$ is allowed. The NLO relation is

$$\begin{aligned} M_{L, L, -}^{m, p(\pi^+)n} &= M_{L, L, -}^{m, n(\pi^-)p} - \left(\frac{L+1}{L} \right) [M_{L, L, +}^{m, p(\pi^+)n} - M_{L, L, +}^{m, n(\pi^-)p}] \\ &+ O(N_c^{-2}) \quad (L \geq 1). \end{aligned} \quad (3.6)$$

A casual glance shows this to be a linear combination of the LO relations in Eq. (3.5); it is the unique combination for which the NLO corrections (in brackets) cancel as well.

One expects this relation to hold empirically a factor of $N_c = 3$ better than its LO counterpart.

Finally, we point out that a number of relations may be obtained from Eq. (2.10) for pure $I = \frac{1}{2}$ or $\frac{3}{2}$ amplitude combinations, but this merely represents a different basis for representing the charge states.

IV. EXPERIMENTAL TESTS

In principle, all seven linear relations included in Eqs. (3.1)–(3.6) (for each allowed value of L), plus the smallness of Eqs. (3.3), can be tested by comparison with available experimental data. The numbers used are the results of partial-wave analysis applied to raw data from experiments in which real photons are scattered off nucleon targets. We use the data presented by the SAID program [22] at George Washington University and the MAID 2003 program [23] at Universität Mainz. Although one requires only a single data set, it is useful to check the extent to which the model dependence of the data analysis used by the two groups affects our comparisons. We find that the difference is not significant for our tests.

It is now convenient to introduce the notation used in the experimental data tables. The *electromagnetic multipoles* are given in terms of our multipole amplitudes:

$$\begin{aligned} M_{L-1,L,-}^e &= +\beta\sqrt{L(L-1)}E_{L-} \\ M_{L+1,L,+}^e &= +\beta\sqrt{(L+2)(L+1)}E_{L+} \\ M_{L,L,+}^m &= -\beta\sqrt{L(L+1)}M_{L+} \\ M_{L,L,-}^m &= -\beta\sqrt{L(L+1)}M_{L-} \end{aligned} \quad (4.1)$$

where [7]

$$\beta \equiv -F_\pi \pi \sqrt{\frac{k_\gamma}{8\pi\alpha}}, \quad (4.2)$$

with $F_\pi \simeq 186$ MeV and k_γ the photon c.m. 3-momentum, is an energy scale that cancels from all linear relations and therefore is irrelevant to this work: From Sec. III, one notes that each term in any one of our linear relations has the same prefactors of β and L entering via Eq. (4.1). The relations therefore take the same form when written in terms of the electromagnetic multipoles. It should also be noted that the convention for the signs of $p(\pi^+)n$ amplitudes appearing in data are often reversed (in MAID, for example) compared to those fixed by the standard Condon-Shortley convention used in this paper.

Before presenting plots comparing our results to data, we pause to consider exactly what suitable agreement among the relations entails. Each partial wave consists of a continuum punctuated by occasional resonances. Of course, the unambiguous separation of these two components is an uncertainty that plagues all partial-wave analyses. Nevertheless, such a separation is routinely performed, and we shall take advantage of such published numerical results.

Our relations should be taken at face value in the continuum regions. Therefore, if the two sides of a relation in such a region are expected to have only $O(1/N_c^2)$ corrections but the agreement is much poorer, then one can say that the relation fails. However, even in such a case, one must question whether the method of extracting the partial wave might be at fault. For example, the $L = 4$ results for Eqs. (3.5) and (3.6) differ greatly between MAID (Fig. 4) and SAID (Fig. 5), with the former much more supportive of our relations; but without further information, one cannot definitively say which scenario is correct. Fortunately, this effect does not occur in most cases.

In the resonant regions, the agreement between amplitudes is much less impressive for a variety of reasons. First, the Δ resonance may appear prominently in some partial waves. However, in large N_c the Δ is not a resonance at all, being a stable partner of the nucleons degenerate in mass up to $O(1/N_c)$ differences. Only because the pion mass is smaller than this difference for $N_c = 3$ is the Δ unstable. There also exist multiplets of true resonances degenerate to mass differences of $O(1/N_c)$ [5], and this will appear as humps in the two sides of relations at relatively shifted positions: For a preview, see the $L = 2$ cases in Figs. 4 and 5. In such cases, we rely upon an analysis introduced in Ref. [8] of comparing the extracted resonant amplitudes directly. Since these quantities are extracted from the full amplitudes with spin- and energy-dependent factors [Eq. (A.3)], it should not be surprising that the raw heights of the resonant bumps in the partial waves are not in exact agreement either; but as we shall see, the agreement of the resonant parameters in this example turns out to be very satisfactory.

In all plots we present both real and imaginary parts of partial wave amplitudes, for values of c.m. energy W of the γN system up to 2 GeV.

We begin with an illustration of the electric multipole results, Eqs. (3.1), (3.2), and (3.3). In Fig. 1 we plot the left-hand side (l.h.s.) and right-hand side (r.h.s.) of Eq. (3.1) for $L = 2-5$, and similarly for Eq. (3.2) with $L = 0-5$ in Fig. 2. It is immediately clear that the relations are convincing, particularly in the energy range below resonances—after all, it has been known for a long time that isoscalar amplitudes are suppressed compared to isovector amplitudes. The $1/N_c$ expansion simply provides an expectation for the relative magnitude of the difference; indeed, the agreement often seems better than $1/N_c$, or 1 part in 3.

Confronting Eq. (3.3) with data is more difficult. One may, for example, superimpose plots of $M_{L\pm 1,L,\pm}^{e,p(\pi^0)p}$ with the corresponding charge-exchange amplitudes and ask whether the former are truly $O(1/N_c)$ smaller than the latter. Since both of these amplitudes have their own unique structure as functions of energy, a sort of averaging procedure is necessary, and a decisive result is not immediately visible. We therefore do not include such plots in

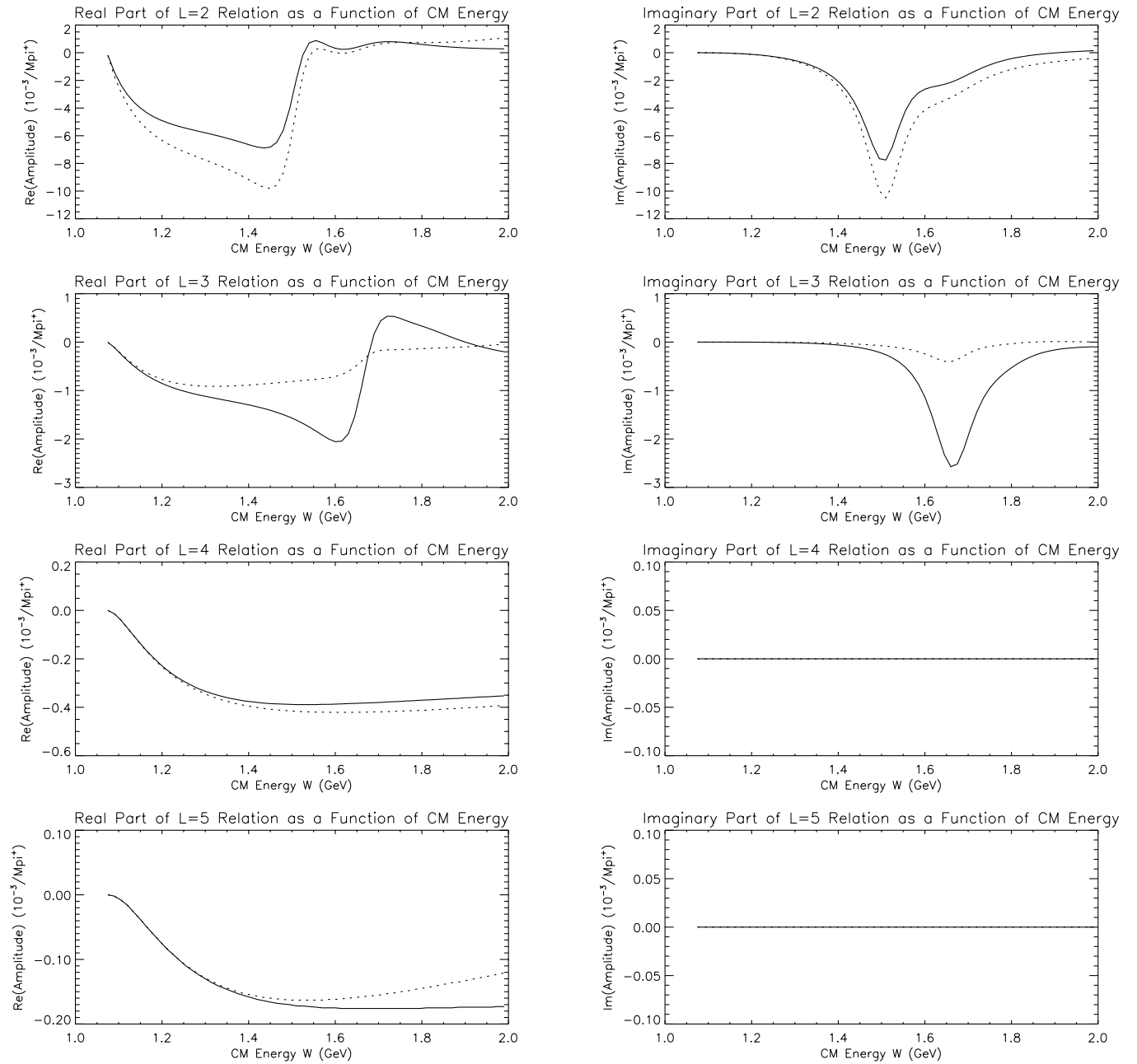


FIG. 1. Electric multipole data from the MAID 2003 website [23]. Solid lines indicate the l.h.s. of relation (3.1) for values $L \geq 2$, while dotted lines represent the r.h.s.

this work. Indeed, there are certain energy regions where the π^0 electric multipoles are actually larger than their charged counterparts, particularly for the imaginary parts in the lower partial waves. By and large, however, the π^0 e amplitudes tend to be smaller at most energies, in general agreement with Eq. (3.3).

We next plot the two sides of the π^0 magnetic relation Eq. (3.4) in Fig. 3 for $L = 1-5$. Agreement for the $L = 1$ partial wave is particularly poor because of the presence of the $\Delta^+(P_{33})$ resonance, which in the large N_c limit is a

stable partner of the nucleons. As L increases, however, one observes an increasingly satisfactory comparison. Even in $L = 2$, where the resonances $D_{13}(1520)$ and $D_{15}(1675)$ appear separated and quite different in amplitude, there is good reason for optimism, as we show below for on-resonance parameters for the charge-changing amplitudes.

Turning now to the charged magnetic multipole relations, we simultaneously test both LO [leftmost of Eq. (3.5)] and NLO [Eq. (3.6)] relations in a single set of

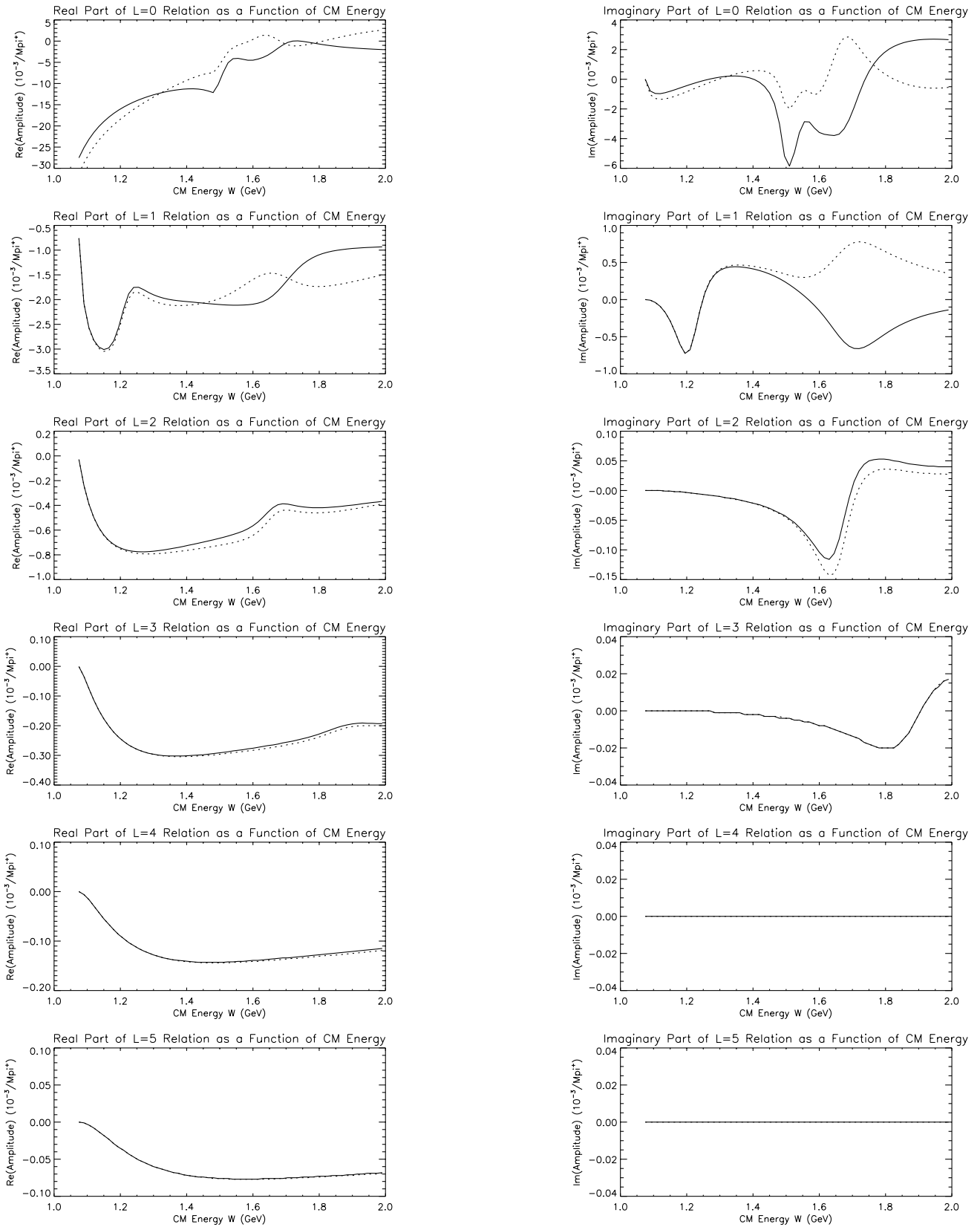


FIG. 2. Electric multipole data from the MAID 2003 website [23]. Solid lines indicate the l.h.s. of relation (3.2) for values $L \geq 0$, while dotted lines represent the r.h.s.

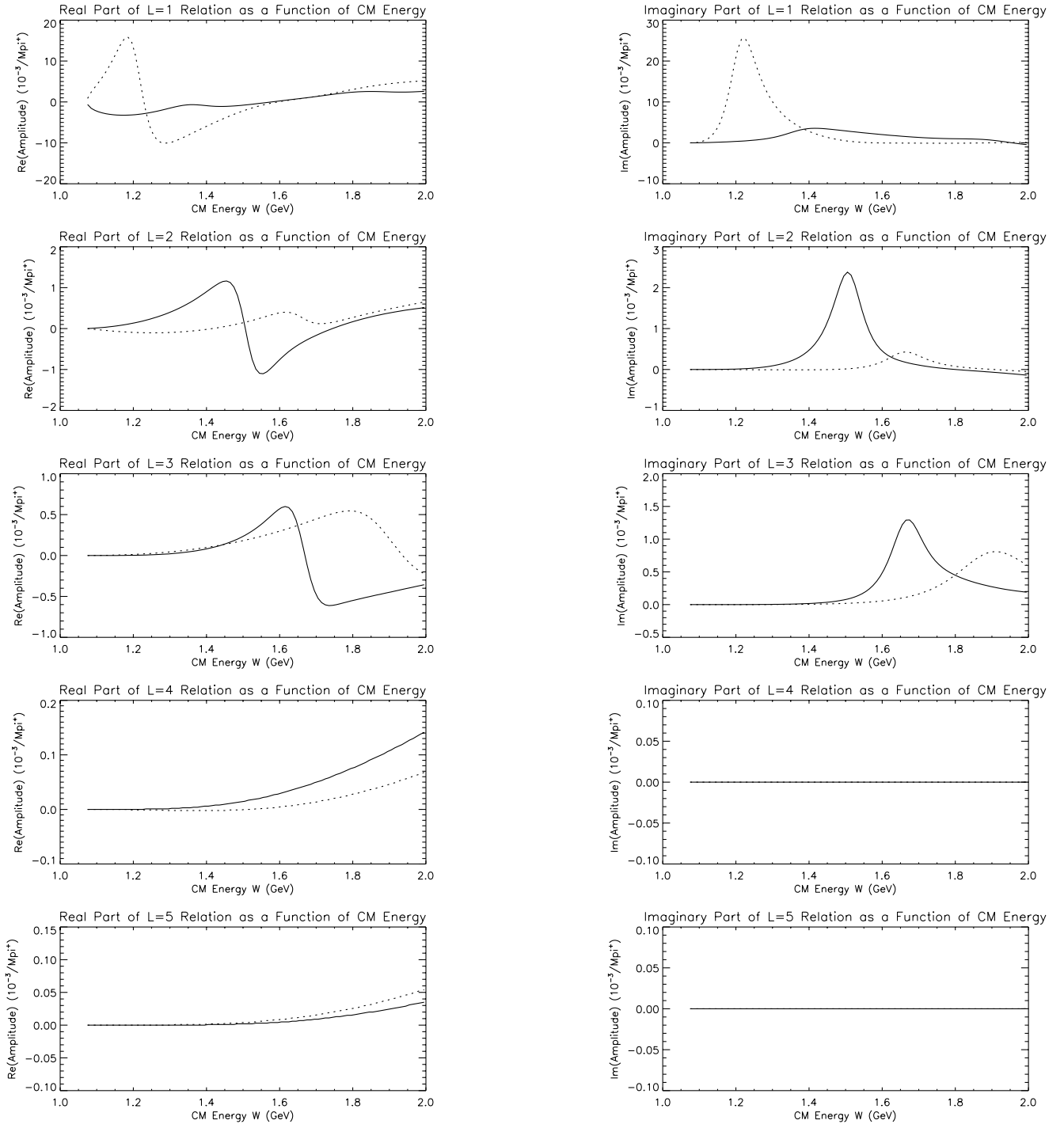


FIG. 3. Magnetic multipole data from the MAID 2003 website [23]. Solid lines indicate the l.h.s. of Eq. (3.4) for values $L \geq 1$, while dotted lines represent the r.h.s.

plots, for $L = 1-5$. In each plot three curves appear, corresponding to $M_{L-}^{p(\pi^+)n}$ [the l.h.s. of Eqs. (3.5) and (3.6)] and the r.h.s.'s of the LO and NLO relations. Since NLO relations are more delicate, we present these combinations using both MAID (Fig. 4) and SAID (Fig. 5) data.

One can infer several interesting conclusions from these figures. First, the LO relations definitely have merit, particularly in the energy range below the appearance of resonances. This is true for all partial waves, real and imaginary parts alike. However, the addition of NLO terms

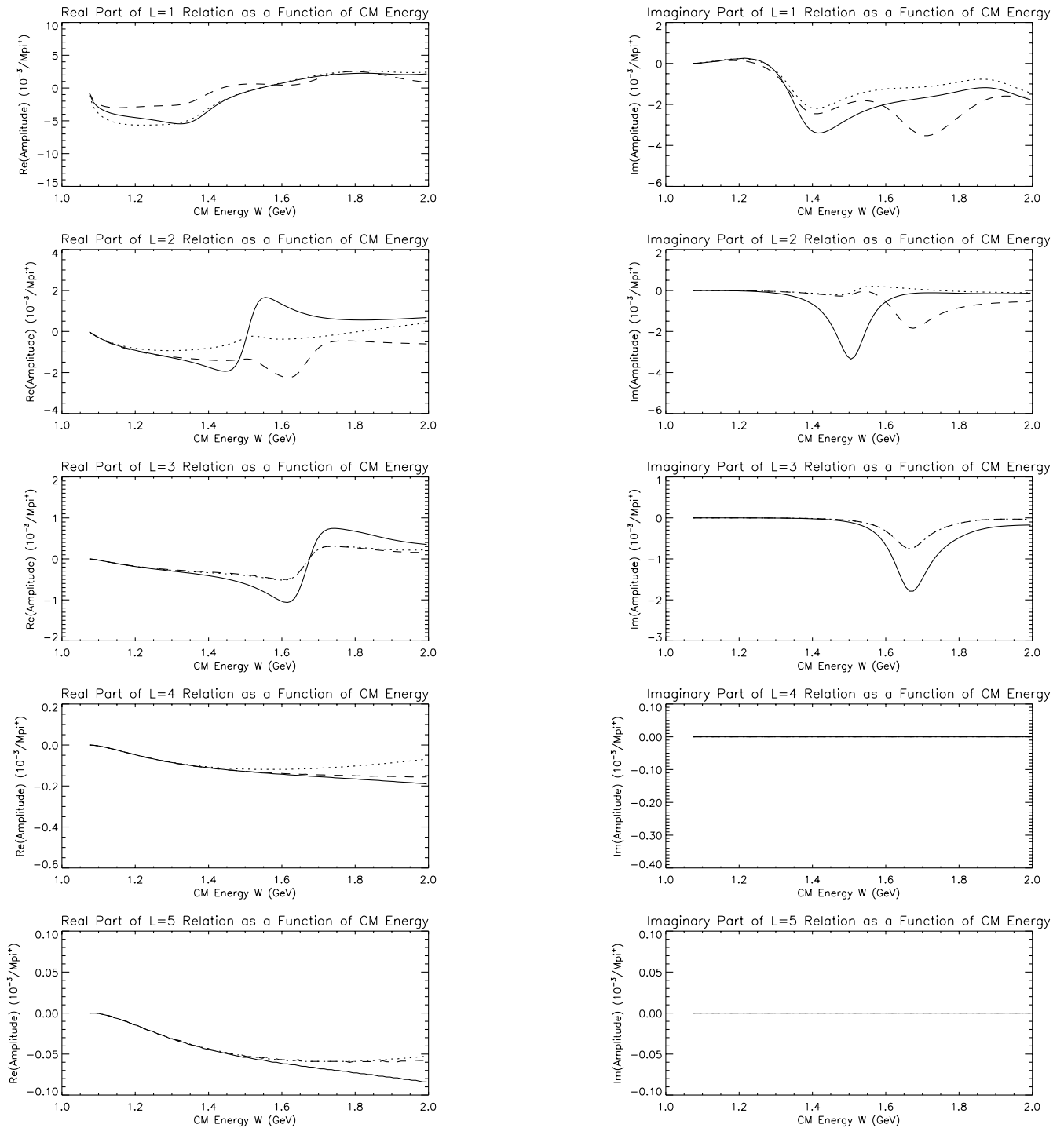


FIG. 4. Magnetic multipole data from the MAID 2003 website [23]. Solid lines indicate the l.h.s. of relations (3.5) and (3.6) for values $L \geq 1$, while dotted lines represent the LO term [first r.h.s. of Eq. (3.5)], and dashed lines include the NLO term in Eq. (3.6).

does not seem to greatly improve agreement between the two curves; indeed, in certain low partial waves (*e.g.*, $L = 1$), the addition of NLO terms seems to make the agreement worse. However, a clue to what is happening may be gleaned from the fact the NLO terms in Eq. (3.6) may

introduce resonances completely absent from the LO terms.

These plots reveal the strong effect of resonances in the lower partial waves on the quality of our predictions. This was noted earlier by Schwesinger *et al.* [8] when they

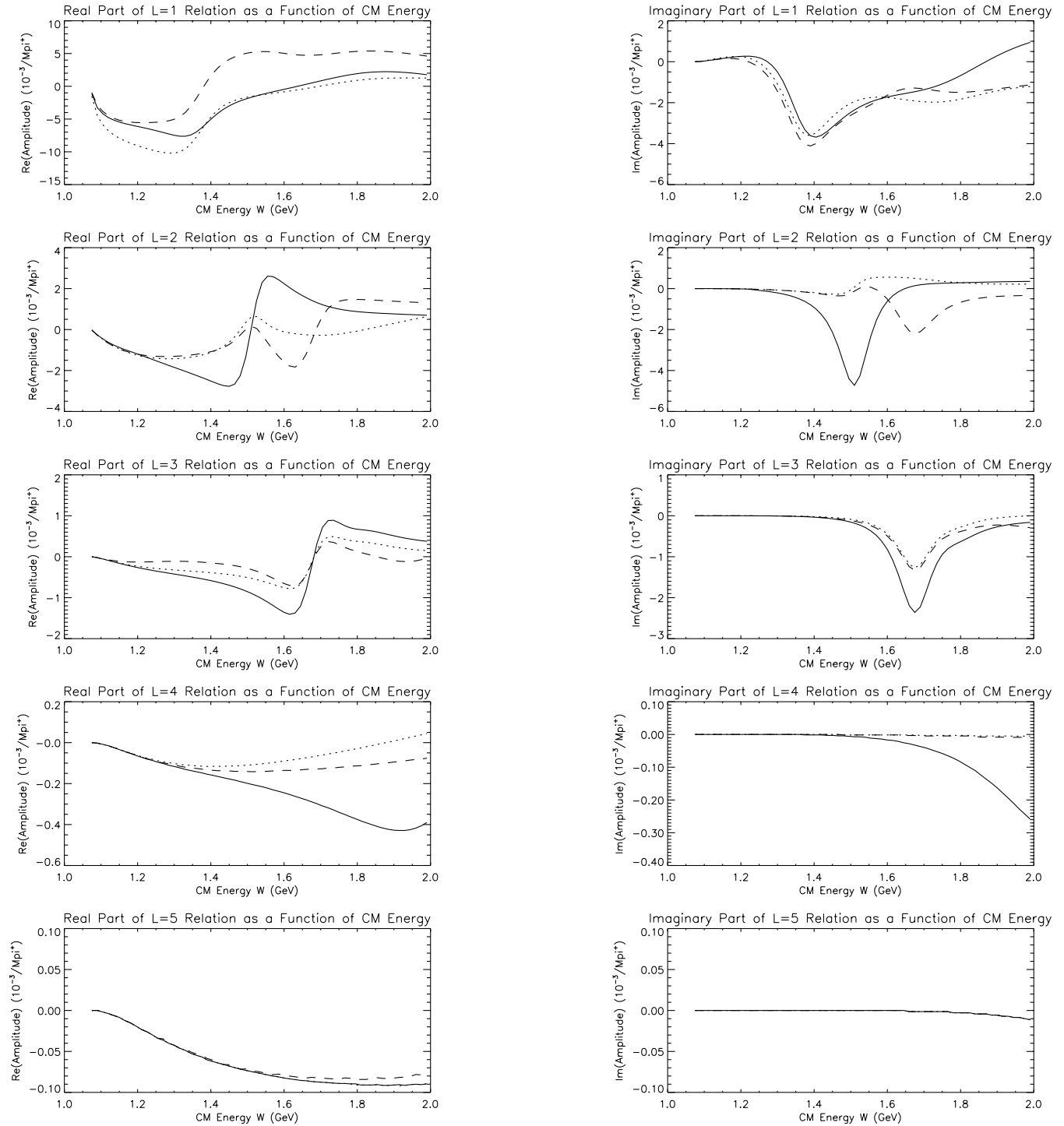


FIG. 5. Magnetic multipole data from the SAID website [22]. Again, solid lines indicate the l.h.s. of the relations (3.5) and (3.6) for $L \geq 1$, while the dotted lines represent the LO term [first r.h.s. of Eq. (3.5)], and dashed lines include the NLO term in Eq. (3.6).

attempted to compare their Skyrme model relations with experiment. Rather than compare the multipole amplitudes along the full energy range, they proposed an alternate testing method using the resonance couplings (obtainable

through the helicity amplitudes) for the relevant resonances.

Such an approach is all the more sensible in the $1/N_c$ expansion, where resonances that would be degenerate in

the large N_c limit may differ in mass by as much as 300 MeV. For example, the Δ - N mass difference is formally only an $O(1/N_c^1)$ effect. One should not be surprised if LO and NLO terms differ by humps that are shifted with respect to each other.

One can proceed in a similar manner to that of Ref. [8], once Eqs. (3.5) and (3.6) are written in terms of the Walker helicity amplitudes [24] A^p , A^n , B^p , and B^n , which are, respectively, proportional to the helicity amplitudes $A_{1/2}^p$, $A_{1/2}^n$, $A_{3/2}^p$, and $A_{3/2}^n$ at each resonance given in the *Review of Particle Properties* [25]. In the present case, each of these amplitudes may have either of $J = L \pm \frac{1}{2}$. The conversion between these amplitudes is outlined in the Appendix; the final result is:

$$[A^p - A^n]_{L-} + \frac{1}{2}(L-1)[B^p - B^n]_{L-} = O(N_c^{-1}), \quad (4.3)$$

$$[A^p - A^n]_{L-} + \frac{1}{2}(L-1)[B^p - B^n]_{L-} + [A^p - A^n]_{L+} - \frac{1}{2}(L+2)[B^p - B^n]_{L+} = O(N_c^{-2}). \quad (4.4)$$

We now consider each partial wave and insert the resonance couplings for nearby $I = \frac{1}{2}$ resonances into the above formulas (paired $I = \frac{3}{2}$ resonances appear to occur too high in energy to significantly influence these plots). After consulting Ref. [25], one sees that only $L = 2$ provides a meaningful test since $D_{13}(1520)$ and $D_{15}(1675)$ can be grouped together as distinct resonances appearing in one of the plotted partial waves. This is fortunate, because the $L = 2$ plot is the most inconclusive of those discussed above. Resonances in other partial waves are either poorly resolved or split too far apart to make a convincing match. We evaluate the l.h.s.'s of Eqs. (4.3) and (4.4), and also show in curly braces the sum of the absolute values of each term to demonstrate the extent of the cancellations. If the $1/N_c$ expression is working, the l.h.s. in the first should be about 1/3 of the corresponding factor in braces, and that in the second should be about 1/9.

$$\text{l.h.s.}(4.3) = -38.4 \pm 5.6 \{100.9\} \times 10^3 \text{ GeV}^{-1} \quad (4.5)$$

$$\text{l.h.s.}(4.4) = -18.2 \pm 8.5 \{140.2\} \times 10^{-3} \text{ GeV}^{-1} \quad (4.6)$$

Expressed as ratios, the results are -0.38 ± 0.06 and -0.13 ± 0.06 , respectively. One sees that the behavior is exactly what one would expect from the $1/N_c$ expansion. Indeed, if anything, the agreement is better than one might expect. For example, a central value in Eq. (4.5) of 20 or 50 would still be acceptable. We conclude that Eq. (3.6) works well, even though the presence of somewhat separated resonances obscures agreement over the full energy range.

V. CONCLUSIONS

We have presented model-independent expressions, derived from the $1/N_c$ expansion of QCD, for pion photoproduction multipole amplitudes. This expansion yields several nontrivial predictions that can be tested with experimental data. We find that the relations holding to leading order in $1/N_c$ match the data quite well in most cases, particularly in the region between threshold and the onset of resonances. The relations holding at next-to-leading order in $1/N_c$ appear to yield a more modest improvement if one insists on considering the amplitudes at all energy scales, including the resonant region. However, when the same relations are employed using parameters extracted directly from distinct resonances appearing in partial waves on the two sides of these equations, the agreement with the expectations of the $1/N_c$ expansion—at both leading and subleading order—is remarkable.

ACKNOWLEDGMENTS

D. C. D. would like to thank E. Beise and J. J. Kelly for explaining the SAID and MAID data. The work of T. D. C. and D. C. D. was supported in part by the U.S. Department of Energy under Grant No. DE-FG02-93ER-40762. The work of R. F. L. and D. R. M. was supported by the National Science Foundation under Grant No. PHY-0140362.

APPENDIX: HELICITY AMPLITUDES

The magnetic multipoles $M_{L\pm}$ can be rewritten in terms of helicity amplitudes. To do this, one introduces the Walker helicity elements [24], $A_{L\pm}$ and $B_{L\pm}$. The labels A and B refer to an initial γN state with total angular momentum $J = L \pm \frac{1}{2}$ that has helicity $\frac{1}{2}$ and $\frac{3}{2}$, respectively. They are related for $L \geq 1$ by [Ref. [24], Eq. (25)]:

$$M_{L+} = \frac{1}{L+1} \left[A_{L+} - \frac{1}{2}(L+2)B_{L+} \right], \quad (A.1)$$

$$M_{L-} = \frac{1}{L} \left[A_{L-} + \frac{1}{2}(L-1)B_{L-} \right]. \quad (A.2)$$

These should be regarded as eight equations, two for each of the four possible pion photoproduction reactions. This is sufficient to obtain Eqs. (4.3) and (4.4).

The Walker helicity elements can be then be written in terms of helicity amplitudes $A_{1/2}^p$, $A_{3/2}^p$, $A_{1/2}^n$, and $A_{3/2}^n$, whose numerical values are tabulated in Ref. [25]. The subscript indicates the helicity of the state, while the superscript indicates the initial nucleon. The relationship between these two representations is given by Eqs. (9.8) and (9.9) of Ref. [8]:

$$\begin{aligned}
\text{Im}A_{L\pm}^{\beta} &= \mp f A_{1/2}^{\beta}, \\
\text{Im}B_{L\pm}^{\beta} &= \pm f \sqrt{\frac{16}{(2J-1)(2J+3)}} A_{3/2}^{\beta}, \\
f &= \sqrt{\frac{1}{(2J+1)\pi} \frac{k_{\gamma}}{k_{\pi}} \frac{M_N}{M_R} \frac{\Gamma_{\pi}}{\Gamma^2}},
\end{aligned} \tag{A.3}$$

where β refers to the initial isospin of the γN system (and therefore subsumes a Clebsch-Gordan coefficient when one refers to a specific nucleon charge state). k_{γ} and k_{π} are the c.m. 3-momenta of the photon and pion, respectively. M_N and M_R are the nucleon and resonance masses, and Γ_{π} and Γ are the pionic and total widths of the resonance, respectively.

-
- [1] T.D. Cohen, D.C. Dakin, R.F. Lebed, and A. Nellore, Phys. Rev. D **70**, 056004 (2004).
- [2] J.-L. Gervais and B. Sakita, Phys. Rev. Lett. **52**, 87 (1984); Phys. Rev. D **30**, 1795 (1984).
- [3] R.F. Dashen and A.V. Manohar, Phys. Lett. B **315**, 425 (1993); **315**, 438 (1993).
- [4] R.F. Dashen, E. Jenkins, and A.V. Manohar, Phys. Rev. D **49**, 4713 (1994).
- [5] T.D. Cohen and R.F. Lebed, Phys. Rev. Lett. **91**, 012001 (2003); Phys. Rev. D **67**, 096008 (2003); Phys. Rev. D **68**, 056003 (2003).
- [6] The leading order in absolute terms is $O(e/\sqrt{N_c})$, but this is irrelevant for our calculations.
- [7] C. Eckart and B. Schwesinger, Nucl. Phys. **A458**, 620 (1986).
- [8] B. Schwesinger, H. Weigel, G. Holzwarth, and A. Hayashi, Phys. Rep. **173**, 173 (1989).
- [9] E. Witten, Nucl. Phys. **B160**, 57 (1979).
- [10] G. Adkins, C. Nappi, and E. Witten, Nucl. Phys. **B228**, 552 (1983).
- [11] T.D. Cohen and R.F. Lebed, Phys. Lett. B **578**, 150 (2004).
- [12] A. Hayashi, G. Eckart, G. Holzwarth, and H. Walliser, Phys. Lett. B **147**, 5 (1984); M.P. Mattis and M. Karliner, Phys. Rev. D **31**, 2833 (1985).
- [13] M.P. Mattis and M.E. Peskin, Phys. Rev. D **32**, 58 (1985); M.P. Mattis, Phys. Rev. Lett. **56**, 1103 (1986); Phys. Rev. D **39**, 994 (1989); Phys. Rev. Lett. **63**, 1455 (1989).
- [14] M.P. Mattis and M. Mukerjee, Phys. Rev. Lett. **61**, 1344 (1988).
- [15] V.B. Berestetskii, E.M. Lifshitz, and L.P. Pitaevskii, *Relativistic Quantum Theory*, (Addison-Wesley, Reading, MA, 1971).
- [16] A.J. Buchmann and R.F. Lebed, Phys. Rev. D **62**, 096005 (2000).
- [17] A.J. Buchmann, J.A. Hester, and R.F. Lebed, Phys. Rev. D **66**, 056002 (2002).
- [18] E. Jenkins, X. Ji, and A. Manohar, Phys. Rev. Lett. **89**, 242001 (2002); R.F. Lebed and D.R. Martin, Phys. Rev. D **70**, 016008 (2004).
- [19] D.B. Kaplan and A.V. Manohar, Phys. Rev. C **56**, 76 (1997).
- [20] A.R. Edmonds, *Angular Momentum in Quantum Mechanics* (Princeton Univ. Press, Princeton, NJ, 1996).
- [21] Of course, this is an empirically testable hypothesis on such data as exists.
- [22] The SAID data is available at George Washington University's Center for Nuclear Studies website: <http://gwdac.phys.gwu.edu>.
- [23] The MAID data is available at the Universität Mainz Institute for Nuclear Physics website: <http://www.kph.uni-mainz.de/maid/>.
- [24] R.L. Walker, Phys. Rev. **182**, 1729 (1969).
- [25] Particle Data Group, Phys. Lett. B **592**, 1 (2004).